Prediction of hip joint load and translation using musculoskeletal modelling with force-dependent kinematics and experimental validation

Journal:	*Part H: Journal of Engineering in Medicine*
Manuscript ID:	JOEIM-14-0205.R3
Manuscript Type:	Original article
Date Submitted by the Author:	12-Apr-2015
Complete List of Authors:	Zhang, Xuan; Stated Key Laboratory for Manufacturing Systems Engineering, School of Mechanical Engineering Chen, Zhenxian; Stated Key Laboratory for Manufacturing Systems Engineering, School of Mechanical Engineering Wang, Ling; Stated Key Laboratory for Manufacturing Systems Engineering, School of Mechanical Engineering Yang, Wenjian; Stated Key Laboratory for Manufacturing Systems Engineering, School of Mechanical Engineering Dichen, Li; Stated Key Laboratory for Manufacturing Systems Engineering, School of Mechanical Engineering Jin, Zhongmin; Stated Key Laboratory for Manufacturing Systems Engineering, School of Mechanical Engineering; Institute of Medical and Biological Engineering, School of Mechanical Engineering
Keywords:	Biodynamics, Gait Analysis, Hip Protheses, Motion/ Posture Analysis, Musculo-Skeletal Mechanics, Hip Biomechanics
Abstract:	Musculoskeletal (MSK) lower limb models are widely used to predict the resultant contact force in the hip joint as a non-invasive alternative to instrumented implants. Previous MSK models based on rigid body assumptions treated the hip joint as an ideal sphere with only three rotational degrees of freedom (DOFs). An MSK model that considered force-dependent kinematics (FDK) with three additional translational DOFs was developed and validated in the present study by comparing it with a previous experimental measurement. A 32-mm femoral head against a polyethylene cup was considered in the MSK model for calculating the contact forces. The changes in the main modelling parameters were found to have little influence on the hip joint forces (RDPV<10 BW%, mean trial deviation<20 BW%). The centre of the hip joint translation was more sensitive to the changes in the main modelling parameters, especially muscle recruitment type (RDPV<20%, mean trial deviation<0.02 mm). The predicted hip contact forces (HCFs) showed consistent profiles, compared with the experimental measurements, except in the lateral-medial direction. The ratio-average analysis, based on the Bland and Altman's plots, showed better limits of agreement (LOA) in climbing stairs (mean LOA: -2.0 to 6.3 in walking, mean LOA: -0.5 to 3.1 in climbing stairs). Better agreement of the predicted HCFs was also found during the stance phase. The FDK approach underestimated the maximum hip contact force by a mean value of 6.68 ±1.75% BW compared with the experimental measurements. The predicted maximum translations of the hip joint centres were 0.125 ± 0.03 mm in level walking and 0.123 ± 0.005 mm in

	climbing stairs.

The recommended reviewers:

Prof. Mark de Zee
Department of Health Science and Technology, Aalborg University
Fredrik Bajers Vej 7, Aalborg East 9220, Denmark
Email: mdz@hst.aau.dk
Phone: 9940 8818

Prof. Markus Wimmer
Department of Orthopedic Surgery, Rush University Medical Center
1611 West Harrison, Suite 204 D, Chicago, IL, 60612, United States.
E-mail: Markus_A_Wimmer@rush.edu
Phone: (312) 942-2789
Fax: (312) 942-2101

Prof. Cheng-Kung Cheng
Orthopaedic Biomechanics Laboratory, Institute of Biomedical Engineering, National Yang Ming University
No.155, Sec.2,Linong St., Shih-Pai, Taipei, 11221 Taiwan
E-mail: ckcheng@ym.edu.tw
Phone: Tel: 886-2-2826-7020
Fax: 886-2-28202519

Prediction of hip joint load and translation using musculoskeletal modelling with force-dependent kinematics and experimental validation

Xuan Zhang[1], Zhenxian Chen[1], Ling Wang (PhD)[1], Wenjian Yang[1], Dichen Li[1], Zhongmin Jin (PhD)[1,2]

1, Stated Key Laboratory for Manufacturing Systems Engineering, School of Mechanical Engineering, Xi'an Jiaotong University, Xi'an, Shaanxi, China

2, Institute of Medical and Biological Engineering, School of Mechanical Engineering, University of Leeds, Leeds, UK, LS2 9JT

Please address all correspondence to:

Dr. Ling Wang

Stated Key Laboratory for Manufacturing Systems Engineering,

School of Mechanical Engineering,

Xi'an Jiaotong University,

Xi'an,

Shaanxi,

China

Email: menlwang@mail.xjtu.edu.cn

Abstract

Musculoskeletal (MSK) lower limb models are widely used to predict the resultant contact force in the hip joint as a non-invasive alternative to instrumented implants. Previous MSK models based on rigid body assumptions treated the hip joint as an ideal sphere with only three rotational degrees of freedom (DOFs). An MSK model that considered force-dependent kinematics (FDK) with three additional translational DOFs was developed and validated in the present study by comparing it with a previous experimental measurement. A 32-mm femoral head against a polyethylene cup was considered in the MSK model for calculating the contact forces. The changes in the main modelling parameters were found to have little influence on the hip joint forces (RDPV<10 BW%, mean trial deviation<20 BW%). The centre of the hip joint translation was more sensitive to the changes in the main modelling parameters, especially muscle recruitment type (RDPV<20%, mean trial deviation<0.02 mm). The predicted hip contact forces (HCFs) showed consistent profiles, compared with the experimental measurements, except in the lateral-medial direction. The ratio-average analysis, based on the Bland and Altman's plots, showed better limits of agreement (LOA) in climbing stairs (mean LOA: -2.0 to 6.3 in walking, mean LOA: -0.5 to 3.1 in climbing stairs). Better agreement of the predicted HCFs was also found during the stance phase. The FDK approach underestimated the maximum hip contact force by a mean value of 6.68 ±1.75% BW compared with the experimental measurements. The predicted maximum translations of the hip joint centres were 0.125 ± 0.03 mm in level walking and 0.123 ± 0.005 mm in climbing stairs.

Keywords: Musculoskeletal model, force-dependent kinematics, Hip contact force, muscle force, Hip joint translation

1. INTRODUCTION

The hip contact force (HCF) in artificial hip joints during locomotion is one of the most important factors in the clinical assessment of gait[1, 2] and preclinical testing of prostheses[3] and as an input for the finite element analysis of stresses and strains in the prosthetic components[4]. Both in vivo and in vitro methods have been developed to investigate HCF during the last century. With in vivo methods, HCF is typically achieved by using radio telemetry devices in the implanted prosthesis[5-7]. However, the in vivo measurement of HCF is cost prohibitive and requires the subject to simultaneously undergo hip arthroplasty, limiting the subjects who can be analysed.

Musculoskeletal (MSK) models have been developed to estimate HCF[8] as an alternative to instrumented prostheses. Various software packages such as OpenSim, LifeModel and AnyBody have been used to estimate HCFs[9-11]. From a physiological point of view, there are 6 degrees of freedom (DOF) in the hip. However, the majority of researchers treat the hip joint as an idealised

3-DOF spherical joint, which does not consider the relative translational motion of the hip joint centre (HJC) of the femoral head with respect to that of the acetabular cup[6, 8]. The hip joint in traditional MSK models also neglects the geometries and the material properties of surrounding tissues, including articular cartilage, and the constraints from the soft tissues such as the capsule ligaments and muscles. These shortcomings limit the applicability of the rigid spherical joint model for understanding more realistic biomechanics in the joint[12, 13]. In light of this, various approaches have been developed to predict HCF while considering the contact geometry of the joint[14, 15]. A force-dependent kinematics (FDK) approach has been introduced recently to overcome the aforementioned shortages of the rigid spherical joint[16]. The FDK approach combines the rigid body dynamics of MSK and elastic contact analysis of the bearing surfaces so that this approach can be potentially used to predict HCFs and muscle forces as well as joint motion simultaneously[17]. However, no detailed and comprehensive studies have applied this new approach to the hip joint. Furthermore, the prediction of HCFs based on the FDK approach needs to be directly validated by experimental data.

The aim of this study was to apply the FDK approach to the hip joint of a full lower limb musculoskeletal model to predict the hip contact force and the hip joint centre translation according to the experimental study[5]. Subsequently, the predicted HCFs were compared against the in vivo measurements[5] for validation.

2. Methods

2.1. Subjects

Level walking at normal speed (average speed: 3.9 km/h) and climbing stairs (three single steps in a 17 cm height) times for three patients with instrumented femoral stems were investigated[18, 19] in this study. The bone dimensions, collected from each patient based on individual CT data, centre of gravity, segment masses and inertia parameters, were used to define the lower limb MSK model (Section 2.3). Although the database had four patients, results for both climbing and walking trials were available in only three of the four patients. Therefore, only three patients were considered in the present study (Table 1).

2.2. Contact model

The hip implant with a 32-mm diameter femoral head against a polyethylene cup was taken from the HIP98 database and adopted in the present study[18]. Because of the lack of details on the polyethylene cup design in the HIP98 database, the common and nominal values of the inner diameter and polyethylene linear thickness[20] were chosen as 32.1 mm and 7.6 mm, respectively. Sensitivity analyses were conducted to determine the influence of key FDK parameters on the predicted HCFs and translations. A nominal inclination angle of 45 degrees was selected for the polyethylene cup. Femoral geometry (anteversion angle, position of the transition point between prosthesis neck and shaft) was implemented based on the HIP98 database. A linear spring element (Figure 1b) that connected the HJCs of the femoral head and the acetabular cup was considered in the software to simulate the passive restriction of the capsule ligaments around the hip joint. The average value of 5×10^4 N/m was adopted as the stiffness of the spring element[21], based on the experimental measurement of capsule ligaments from healthy subjects. For THR patients, lower values were also assumed in the present study to simulate the injuries to the capsule ligaments in a sensitivity analysis of the stiffness values.

Hip contact forces predicted by the FDK approach were based on the contact between two surfaces (cup inner surface and femur head surface) in STL format. A linear force-penetration volume law was adopted to calculate the contact force between the two surfaces using a *PressureModule* parameter in N/m^3 and the commercial software AnyBody (Version 6.0, Anybody Technology, Aalborg, Denmark)[22]. This contact model in AnyBody was similar to the elastic foundation theory for the polyethylene cup[23] and tibial insert[24]. Accordingly, the following equation (Eq 1) was adopted to define the *PressureModule* for the polyethylene cup:

$$PressureModule = \frac{pA}{dA} = \frac{E\left[\frac{1}{1-2v} + \frac{2}{1+v}\left(\frac{R_2}{R_1}\right)^3\right]}{R_1\left[\left(\frac{R_2}{R_1}\right)^3 - 1\right]} \tag{1}$$

where *A* is unit contact area and *pA* and *dA* are the contact pressure and penetration depth on each unit area, respectively. The main parameters investigated were the radius of the inner cup surface (R_1), the radius of the outer cup surface (R_2), the elastic modulus (E) and Poisson's ratio (v) of the polyethylene cup. A single elastic modulus value of 850 MPa and a Poisson's ratio of 0.4 for the polyethylene cup were adopted in the present study[25]. The thickness of the UHMWPE cup directly influenced the *PressureModule* value. The effects of using different thicknesses of the UHMWPE cup under the same radius of inner cup surface were investigated. The maximum, minimum and average thicknesses were 14.11 mm, 5.72 mm, and 7.60 mm, respectively [20], resulting in *PressureModule* values of 4.42×10^{11} N/m^3, 2.56×10^{11} N/m^3 and 2.88×10^{11} N/m^3.

2.3. Musculoskeletal model

In the present study, the lower extremity musculoskeletal model was adopted from the commercial MSK simulation software AnyBody (Version 6.0, Anybody Technology, Aalborg, Denmark), which was based on the Twente Lower Extremity Mode[26]. Only the left limb was considered for the MSK model. The actuators that drove the model body segment that acted on the pelvis with respect to the global reference system were used to balance the missing contralateral leg during the simulation[27]. The trial data were mirrored for the patient with a right-implanted prosthesis.

The MSK model with the FDK approach in the present study consisted of the pelvis, thigh, patella, shank and foot segment. The length and mass of each lower limb segment were manually set for the three patients according to the values published by Heller et al.[3] and the HIP98 database. The unilateral model included 8 joints. Revolute joints were applied for the knee, ankle, and subtalar joints. The knee was allowed to move in the flexion/extension direction; the ankle moved in the sagittal plane and was constrained for all others; and the subtalar joint moved in the eversion/inversion direction. The implanted hip joint was represented as a full 6 degrees of freedom hip joint in the FDK approach[16] (Figure 1). The coordinate system of the hip joint on the femoral head is shown as follows (Figure 1a): the anterior-posterior direction in the sagittal plane, the lateral-medial direction in the transverse plane and perpendicular to the sagittal plane, and with the superior-inferior direction being the intersecting line between the coronal and sagittal planes. The coordinate systems of the other segments were in accordance with the International Society of Biomechanics[28]. The lower limb MSK model contained approximately 160 muscle units. Muscle attachment points were linearly scaled according to the research by Klein Horsman[26] and adjusted for each patient. The muscle isometric strength F_{ISO} was assumed to be proportional to the physiological cross-sectional area using a constant of 37 N/cm^2[29]. Three muscle recruitment criteria were considered in the sensitivity analysis: the quadratic polynomial criterion, cubic polynomial criterion, and min/max criterion. The differences between each muscle recruitment criteria were described in the literature[30] (Table 2). The quadratic polynomial and cubic polynomial criteria were adopted from a previous study[27] (power of the objective function p=2, p=3). For the purpose of comparing the calculated HFCs and the experimental measurements, joint angles and pelvis position from the HIP98 database were used to drive the MSK model. Ground reaction forces were applied to predict muscle forces and HCFs. The same MSK model without FDK was also adopted to investigate the difference between the 6-DOF MSK model and the conventional 3-DOF model.

HCFs calculated from the MSK model with the FDK approach were compared with the experimental measurements from the HIP98 database. The predicted HCFs were resolved into three anatomical directions. The relative deviation of peak value (RDPV) for the resultant force (as a percentage of the experimental peak) and the average trial deviation (the average difference between the experimental and predicted HCFs through each trial) were used to assess the differences in peak HCF values and the variations during an entire gait cycle. Bland and Altman's 95% limits of agreement (LOA)[31] and the root mean square error (RMSE) were calculated to facilitate the comparison. The difference-average and ratio-average of Bland and Altman's plots were not only used to investigate the agreement of the FDK approach compared with the experimental measurement, but also used to investigate the difference of predicted HCFs between swing and stance phases in a gait.

No information on muscle EMGs was available from the HIP98 database. As an alternative, a qualitative comparison was made between the present prediction and the previous studies of EMG profiles for normal healthy subjects for both level walking[32] and stair climbing[33]. The predicted muscle forces under level walking and climbing stairs were all from Subject S1. Only six muscles that crossed the hip were considered for level walking: *the gluteus maximus (12 bundles), gluteus medius (12 bundles), adductor longus (6 bundles), semitendinosus (single bundle), biceps femoris caput longum (single bundle)* and *rectus femoris (2 bundles)*. Four muscles were considered for climbing stairs: the *gluteus maximus (12 bundles), gluteus medius (12 bundles), rectus femoris (2* *bundles)* and *semitendinosus (single bundle).*

Translation of HJC was calculated as the linear distances between the centres of the acetabular cup and the femoral head. The origin of the local acetabular coordinate system was constructed in the same manner as the femoral head to calculate HJC translation. A vector from the origin of the acetabular coordinate system to the HJC of the femoral head in the local acetabular coordinate system was calculated as the hip centre translation. The average values of the predicted translations were transformed to the acetabular coordinate system, as defined in the study by Tsai et al[34]. In this system, the anterior-posterior direction was parallel to the interception line of the cup opening and sagittal planes. The in-out direction was the normal vector of the cup opening plane. The lateral-medial direction was perpendicular to the other two directions. The predicted translations were compared with their experimental study of 28 THAs (32 to 36 mm diameters) using a dual fluoroscopy system.

A sensitivity analysis was performed for the input modelling parameters on the predictions of both the HCF and HJC translations. These parameters were muscle recruitment, muscle insertion sites, *PressureModule*, stiffness of spring element and type of actuator. The muscle insertion sites were altered by 5 mm and 10 mm in the A-P, S-I and L-M directions for each of the four muscles around the hip joint in turn[35].

3. Results

Similar trends to those of the predicted HCFs were found with the experimental measurements (Figure 2). Furthermore, the predicted HCFs were lower than the experimental measurements during the swing phase, especially under level walking (Figure 2). The FDK approach overestimated the HCFs at peak value, except for Subject S3 (Table 3). The mean trial deviations of the HCFs had negative values, indicating that the FDK approach underestimated the HCFs in all trials. The predicted HCFs showed consistent profiles, compared with the experimental measurements in the anterior-posterior (A-P) direction (Figure 3a, b) for all trials. Similar trends were also found in the superior-inferior (S-I) direction, where the profiles of the predicted HCFs in the S-I direction were similar to the resultant HCFs. In the A-P direction, the profiles of the predicted HCFs were closer to the experimental values for climbing stairs than for level walking, especially at the first peak value. The numerical results of the HCFs showed that the mean trial devia\tions were positive, indicating that the FDK approach overestimated the HCF measurements in the A-P and M-L directions (Table 4). However, the predicted HCFs showed large differences compared with the experimental values in the lateral-medial (L-M) direction (Figure 3c, d). There were few differences in the predicted HJCs between the 6-DOF MSK model and the conventional 3-DOF model. The difference in the peak values was less than 5%. In the Bland-Altman plots of the HCFs (Figure 7), over 90% of points were within the upper and lower bounds of 1.96 standard deviation in two analyses. In the difference-average analysis (Figure 7a, b), the mean values of LOA were from -53.6 to 99.1 BW% in level walking and from -62.2 to 97.7 BW% in climbing stairs. In the ratio-average analysis (Figure 7c, d), the mean LOA values were from -2.0 to 6.3 in walking and from -0.5 to 3.1. In the ratio-average analysis, the ratio value converged to the solid line (mean difference value) while the mean values were above 150 BW%.

From the sensitivity analysis, the relative deviation of the peak value and the average trial deviation suggested that the predicted HCFs were rather insensitive to the changes in these input parameters (Table 2). The radial clearance between the polyethylene cup and the femoral head also had a small effect on the predicted HCFs (< 5%). All other modelling variables had only a minor influence on the predicted HCFs. The RDPV and mean trial deviation were less than 10% and 20% BW, respectively. The hip joint translation was more sensitive to the changes in the modelling parameters, especially for the muscle recruitment type (RDPV<20%, mean trial deviation<0.02 mm). More details on the sensitivity analysis are provided in the Appendix.

The predicted muscle forces were compared with the experimental EMG data under level walking and climbing stairs for Subject S1 (Figure 4). The activities of the predicted multi-bundle muscles, such as the *gluteus maximus* and *gluteus medius*, were consistent with the EMG data. The *adductor longus* and *rectus femoris muscles* had better agreement with the experimental data in climbing stairs than in level walking.

The HJC translation had a large variation during the swing phase (Figure 5). The predicted translations in the L-M and S-I directions were positive during the stance phase and negative during the swing phase. The maximum values of the predicted HJC translations occurred during the swing phase, except for climbing stairs for S3. The maximum values were 0.125 ± 0.03 mm for level walking and 0.123 ± 0.005 mm for climbing stairs. The predicted translation tended to the lateral and inferior direction during the swing phase, and the muscles around the hip joint generated minimum forces to pull the femoral head. Figure (6) attempts to compare the qualitative trends in the predicted HJC translations with the experimental measurements given that there were many differences between the computational and experimental studies, as explained in Section (2). Under the acetabular coordinate system defined in the study by Tsai et al[34], the translations trended in the posterior direction at heel strike and the anterior direction at toe off during the stance phase in both the predicted and the experimental data. In the other two directions (in-out, lateral-medial), the translations were towards the acetabular cup and in the medial direction during the stance phase in both the predicted and experimental data. The opposite trend was found (away from the cup and in the lateral direction) during the swing phase. The predicted translations of the hip joint centre were of the same order of magnitude as the experimental measurement[34]. The ranges of the predicted average translations were -0.034 to -0.001 mm in the A-P direction (-0.031 to 0.032 mm in the experiment), -0.041 to 0.061 mm in the in-out direction (-0.075 to 0.061 mm in the experiment) and -0.024 to 0.036 mm in the L-M direction (-0.096 to 0.036 mm in the experiment) (Figure 6). The correlation coefficients between the predicted translations and the experimental measurements were 0.61, 0.43 and 0.52 in each component directions.

4. Discussion

A new FDK approach was applied to the hip joint of a lower limb MSK model to predict the HCFs and to validate through experimental measurements in the present study. This model enabled the consideration of the articular surface geometry, the material properties and the influence between the forces and kinematics of the hip joint centre at the same time. The translation of the hip joint centre could therefore be predicted based on this approach. To the authors' knowledge, no previous studies have reported an explicit deformable articular hip joint model in a full lower limb MSK model and compared the corresponding predictions with experimental measurements.

Compared with the conventional 3-DOF model, the present FDK approach did not show large differences in the prediction of HCFs (< 5%). However, there are two main advantages of using the FDK approach in this research. First, three additional translational DOFs were predicted, in comparison with a conventional ideal spherical hip joint model. This consideration addressed the influences between the forces and the kinematics of the hip joint and therefore may have the potential to investigate certain clinical problems such as micro-separation, dislocation and impingement after validation by experiment.

Second, previous MSK models that took into account the geometry of artificial hip implants and their material properties only considered the hip joint and neglected neighbouring joints and the muscles across the hip in the lower extremity. Considering these factors, the model in this study established a full lower extremity MSK model with the consideration of a hip implant. Therefore, it is possible to investigate hip implants in a more realistic MSK environment. The present study provided additional information about applying the FDK approach to the hip joint compared with the previous study by Andersen et al[16], by considering the *PressureModule* formulation, the sensitivity analysis of different parameters, etc.

The computational prediction of the hip joint load depended on a number of input parameters. Therefore, a parametric analysis was performed to examine the sensitivity of these parameters on the predicted joint loading. The quadratic polynomial muscle recruitment criterion, which showed superior prediction of HCFs, was adopted for the purpose of comparison with similar studies[27, 36]. For the comparison with previous literature[27], quadratic polynomial muscle recruitment was adopted in the MSK model. Few differences in the predicted HCFs and translations were found in the sensitivity analysis of the muscle recruitment criteria. The muscle insertion sites scarcely influenced the predicted HCF and HJC translations. Only a 10-mm deviation in the gluteus medius resulted in a 9.16% change in RDPV in the HJC translation. The sensitivity of the UHMWPE cup thickness had little effect on the predicted HCF and the translation of the HJC. Therefore, the detailed consideration of the cup design, such as cup thickness, would not have much influence. A simple linear spring element with average stiffness was adopted in the present model to represent the restriction of the capsule ligaments around the hip joint[21]. The effect of the ligament on the predicted HCF and HJC translations was small when the stiffness value was reduced to reflect the potential damage from surgery.

The HCFs in the S-I and A-P directions that were predicted by the FDK approach were also found to be consistent with the profiles of the experimental measurements, particularly the A-P component. Although the HCFs in the A-P were relatively small parts of the resultant force, this component was still important. The present MSK model accurately predicted HCFs in the A-P direction, and this may be important when considering the lubrication of the hip joint[37], anterior hip pain and subtle hip instability. However, the FDK approach was unable to predict the HCFs in the L-M direction with similar accuracy. This result was consistent with a previous, similar study (using the HIP98 database) that found greater differences between the predicted HCFs and the experimental measurements in the L-M direction[36]. Bland-Altman plots are usually used to examine by how much the new method is likely to differ from the old in trend and magnitude. Although Bland and Altman's plots are widely used in the comparison between two methods, it has seldom been reported in the validation of musculoskeletal models, especially for the prediction of HCFs. Over 90% of data points were within the range of LOA in two analyses. The majority of the data points out of the range of LOA were during the swing phase of gait, which showed worse agreement of the prediction than the stance phase. The data points in the difference-average analysis were above the solid line (mean difference value) while the mean values were lower than 150 BW% (walking: S1, S2, S3;

climbing stairs: S1). This indicated that the FDK approach underestimated the HCFs at the beginning of and after the toe off in a gait cycle. The opposite tendency was found while the mean values were higher than 150 BW%. All these observations were in accordance with the profiles of the predicted HCFs. The data points in the ratio-average analysis were converged to the solid line (mean ratio value) while the mean values were higher than 100 BW% (walking: S1, S2, S3; climbing stairs: S1, S3). These results indicated that the predicted HCFs by the FDK approach were more accurate during the stance phase in a gait cycle, consistent with the predicted profiles.

It is impossible to directly measure muscle forces in vivo for validation. To validate the MSK model, the predicted HCFs were compared against EMG signals that were recorded in healthy subjects. This type of validation can be found in previous studies[7, 27] and should be considered with caution. Previous studies[38, 39] have shown that patient gait and EMG patterns were observed to shift toward normality, although hip muscle weakness could still persist. The predicted muscle forces were compared indirectly with the EMG profiles from another study on normal subjects,[32, 33] and consistent profiles were found with experimental values during the stance phase, especially for the multi-bundle muscles (*gluteus maximus*, *gluteus medius*). However, the forces of the *biceps femoris, caput longum* and *semitendinosus* were 30% less than the results in a similar study[27]. This might have been caused by the differences in the scaling of the muscle attachment points. Although this comparison was qualitative, it was still meaningful. The muscle attachment points from individual patients were not readily available from the experimental database. We scaled the cadaveric model to define the muscle attachment point for each patient. The predicted muscle forces had poor agreement during the swing phase. Similar results (polynomial muscle recruitment criterion with the power of p=2) were also found in a study by Modenese et al.[27] Muscle synergism is enhanced by increasing the power of p in the polynomial recruitment criterion. With the lower power of objective function (p<5), the muscle might be less sensitive under small external loading. Modenese et al.[27] found that the predicted muscle forces with higher powers of objective function (p=5) had better agreement during the swing phase. However, the overall predicted muscle forces showed better performance during the whole cycle, whereas the power of objective function was two.

The HJC translation had greater variation during the swing phase than the stance phase. The predicted translation indicated that the femoral head moved to the lateral and inferior directions during the swing phase but that the muscles around the hip joint generated minimum forces to pull the femoral head. The maximum hip translation was measured as 0.45 ± 0.09 mm during the swing phase by dual fluoroscopy[34], much larger than the present prediction (0.125 ± 0.03 mm in level walking and 0.123 ± 0.005 mm in climbing stairs). However, the similar tendency of the profiles can be found by comparing the average values. It should be highlighted that the average HJC translation values using dual fluoroscopy contained both positive and negative signs, which resulted in much lower average values than the resolution of the dual fluoroscopy system. Furthermore, large variations in the experimental measurements were observed. Although some of these variations could be attributed to the variations in patients, improved measurement accuracy is also required. Nevertheless, the average HJC translations between the computational predictions and the experimental measurements were of the same orders of magnitude. Although this comparison was qualitative in nature, it still showed the potential of the FDK approach for predicting joint centre kinematics.

This study still possessed a number of limitations. First, the muscle attachment points of this MSK model were linearly scaled, based on the anatomy data, which could have introduced error in the prediction of muscle forces. Therefore, more realistic scaling methods should be applied to the MSK model to more accurately predict muscle forces. Second, video fluoroscopy has been used to measure kinematics, especially in vivo translations of the hip joint[40]. However, this method is difficult to apply to different over-ground gait trails such as climbing stairs, etc., and it is expensive. Although the use of skin markers in motion analysis does not provide a direct measurement of the hip translation, MSK modelling with the FDK approach has the potential to address this issue. It should be noted that the predicted HJC translations were not directly validated by experiments in the present study. Quantitative validation using experimental measurements for predicting translations should be performed in the next step. Despite these limitations, the MSK model with the FDK approach still has the potential to predict realistic HCFs and hip joint kinematics and can be applied to examine a number of surgical and design parameters.

5. Conclusions

In conclusion, a successful multi-body dynamics model of the lower MSK with the consideration of force-dependent kinematics was developed and applied to an artificial hip joint. This MSK model fully considered 6-DOF of the hip joint and was able to predict the hip contact and muscle forces simultaneously. Overall, consistent profiles were found between the predicted hip contact forces and the experimental measurements, particularly in the superior-inferior and anterior-posterior directions. The MSK model with the FDK approach also had the potential to predict the HJC translation. However, this methodology needs to be validated in future studies.

6. Acknowledgments

This work was supported by The Fundamental Research Funds for the Central Universities, Natural Science Foundation of China [grant number 51205303, 51323007], the National Science and Technology Supporting Program [grants number 2012BAI18B00], and the program of Xi'an Jiaotong University [grant number xjj2012108].

7. Conflict of Interest

We confirm that there are no known conflicts of interest associated with this publication, and there has been no significant financial support for this work that could have influenced its outcomes.

8. References

1. Jonkers I, Stewart C, Spaepen A. The study of muscle action during single support and swing phase of gait: clinical relevance of forward simulation techniques. *Gait & Posture*. 2003; 17: 97-105.
2. Steele KM, Seth A, Hicks JL, Schwartz MS, Delp SL. Muscle contributions to support and progression during single-limb stance in crouch gait. *Journal of Biomechanics*. 2010; 43: 2099-105.
3. Heller MO, Bergmann G, Deuretzbacher G, et al. Musculo-skeletal loading conditions at the hip during walking and stair climbing. *Journal of Biomechanics*. 2001; 34: 883-93.
4. Kunze M, Schaller A, Steinke H, Scholz R, Voigt C. Combined multi-body and finite element investigation of the effect of the seat height on acetabular implant stability during the activity of getting up. *Computer Methods And Programs In Biomedicine*. 2012; 105: 175-82.
5. Bergmann G, Deuretzbacher G, Heller M, et al. Hip contact forces and gait patterns from routine activities. *Journal of Biomechanics*. 2001; 34: 859-71.
6. Rydell NW. Forces acting on the femoral head-prosthesis. A study on strain gauge supplied prostheses in living persons. *Acta orthopaedica Scandinavica*. 1966; 37: Suppl 88:1-132.

7. Stansfield BW, Nicol AC, Paul JP, Kelly IG, Graichen F, Bergmann G. Direct comparison of calculated hip joint contact forces with those measured using instrumented implants. An evaluation of a three-dimensional mathematical model of the lower limb. *Journal of Biomechanics*. 2003; 36: 929-36.

8. Brand RA, Crowninshield RD, Wittstock CE, Pedersen DR, Clark CR, Vankrieken FM. A MODEL OF LOWER-EXTREMITY MUSCULAR ANATOMY. *Journal of Biomechanical Engineering-Transactions of the Asme*. 1982; 104: 304-10.

9. Delp SL, Anderson FC, Arnold AS, et al. OpenSim: open-source software to create and analyze dynamic Simulations of movement. *Ieee Transactions on Biomedical Engineering*. 2007; 54: 1940-50.

10. Manders C, New A, Rasmussen J. Validation of musculoskeletal gait simulation for use in investigation of total hip replacement. *Journal of Biomechanics*. 2008; 41: S488.

11. Sherman MA, Seth A, Delp SL. Simbody: multibody dynamics for biomedical research. In: McPhee J, Kovecses J, (eds.). *Iutam Symposium on Human Body Dynamics*2011, p. 241-61.

12. Brandt K, Radin E, Dieppe P, Van De Putte L. Yet more evidence that osteoarthritis is not a cartilage disease. *Annals of the rheumatic diseases*. 2006; 65: 1261-4.

13. Stops A, Wilcox R, Jin Z. Computational modelling of the natural hip: a review of finite element and multibody simulations. *Computer methods in biomechanics and biomedical engineering*. 2012; 15: 963-79.

14. Bei Y, Fregly BJ. Multibody dynamic simulation of knee contact mechanics. *Medical engineering & physics*. 2004; 26: 777-89.

15. Genda E, Iwasaki N, Li G, MacWilliams BA, Barrance PJ, Chao E. Normal hip joint contact pressure distribution in single-leg standing—effect of gender and anatomic parameters. *Journal of Biomechanics*. 2001; 34: 895-905.

16. Andersen MS, Damsgaard M, Rasmussen J. Force-dependent kinematics: a new analysis method for non-conforming joints. *13th Biennial International Symposium on Computer Simulation in Biomechanics*2011.

17. Andersen MS, Rasmussen J. Total knee replacement musculoskeletal model using a novel simulation method for non-conforming joints. *International Society of Biomechanics Conference*2011.

18. Bergmann G, Graichen F, Rohlmann A. Hip joint loading during walking and running, measured in two patients. *Journal of biomechanics*. 1993; 26: 969-90.

19. Bergmann G, Graichen F, Siraky J, Jendrzynski H, Rohlmann A. Multichannel strain gauge telemetry for orthopaedic implants. *Journal of Biomechanics*. 1988; 21: 169-76.

20. Jin Z, Heng S, Ng H, Auger D. An axisymmetric contact model of ultra high molecular weight polyethylene cups against metallic femoral heads for artificial hip joint replacements. *Proceedings of the*

Institution of Mechanical Engineers, Part H: Journal of Engineering in Medicine. 1999; 213: 317-27.

21. hewitt j, guilak f, glisson r, vail tp. regional material properties of the human hip joint capsule ligaments. *jornal of orhoad rarh*. 2001: 359-64.

22. AnyBody. "Anyscript Reference Manual/AnyForceSurfaceContact". *Anybody Technology, Aalborg, Denmark*.

23. Jin Z, Dowson D, Fisher J. A parametric analysis of the contact stress in ultra-high molecular weight polyethylene acetabular cups. *Medical engineering & physics*. 1994; 16: 398-405.

24. Fregly BJ, Bei Y, Sylvester ME. Experimental evaluation of an elastic foundation model to predict contact pressures in knee replacements. *Journal of biomechanics*. 2003; 36: 1659-68.

25. Hua X, Wroblewski BM, Jin Z, Wang L. The effect of cup inclination and wear on the contact mechanics and cement fixation for ultra high molecular weight polyethylene total hip replacements. *Medical Engineering & Physics*. 2012; 34: 318-25.

26. Horsman K, Koopman H, Van der Helm F, Prosé LP, Veeger H. Morphological muscle and joint parameters for musculoskeletal modelling of the lower extremity. *Clinical Biomechanics*. 2007; 22: 239-47.

27. Modenese L, Phillips AT, Bull AM. An open source lower limb model: Hip joint validation. *J Biomech*. 2011; 44: 2185-93.

28. Wu G, Siegler S, Allard P, et al. ISB recommendation on definitions of joint coordinate system of various joints for the reporting of human joint motion—part I: ankle, hip, and spine. *Journal of biomechanics*. 2002; 35: 543-8.

29. Haxton H. Absolute muscle force in the ankle flexors of man. *The Journal of physiology*. 1944; 103: 267-73.

30. Rasmussen J, Damsgaard M, Voigt M. Muscle recruitment by the min/max criterion—a comparative numerical study. *Journal of Biomechanics*. 2001; 34: 409-15.

31. Bland JM, Altman D. Statistical methods for assessing agreement between two methods of clinical measurement. *The lancet*. 1986; 327: 307-10.

32. Wootten M, Kadaba M, Cochran G. Dynamic electromyography. II. Normal patterns during gait. *Journal of Orthopaedic Research*. 1990; 8: 259-65.

33. McFadyen BJ, Winter DA. An integrated biomechanical analysis of normal stair ascent and descent. *Journal of biomechanics*. 1988; 21: 733-44.

34. Tsai T-Y, Li J-S, Wang S, Scarborough D, Kwon Y-M. In-vivo 6 degrees-of-freedom kinematics of metal-on-polyethylene total hip arthroplasty during gait. *Journal of biomechanics*. 2014; 47: 1572-6.

35. Pellikaan P, van der Krogt M, Carbone V, et al. Evaluation of a morphing based method to estimate

muscle attachment sites of the lower extremity. *Journal of biomechanics*. 2014; 47: 1144-50.

36. Modenese L, Phillips ATM. Prediction of hip contact forces and muscle activations during walking at different speeds. *Multibody Syst Dyn*. 2012; 28: 157-68.

37. Wang F, Jin Z. Transient elastohydrodynamic lubrication of hip joint implants. *Journal of Tribology*. 2008; 130: 011007.

38. Long WT, Dorr LD, Healy B, Perry J. Functional recovery of noncemented total hip arthroplasty. *Clinical Orthopaedics and Related Research*. 1993; 288: 73-7.

39. Murray M, GORE DR, BREWER BJ, MOLLINGER LA, SEPIC SB. Joint function after total hip arthroplasty: a four-year follow-up of 72 cases with Charnley and Mtiller replacements. *Clinical orthopaedics and related research*. 1981; 157: 119-24.

40. Lombardi Jr AV, Mallory TH, Dennis DA, Komistek RD, Fada RA, Northcut EJ. An< i> in vivo</i> determination of total hip arthroplasty pistoning during activity. *The Journal of Arthroplasty*. 2000; 15: 702-9.

Fig 1. The schematic of MSK model by the FDK approach. (a) The FDK approach provided three additional translation DOFs in hip joint (anterior-posterior, superior-inferior and medial-lateral direction). (b) A linear spring element was used to simulate the passive function of capsule ligaments.

Fig 2. Comparison between the HCFs of FDK approach (in blue) and experimental HCFs (in red) for (a) level walking and (b) stair climbing.

Fig 3. Comparison between the HCFs of FDK approach (in blue) and experimental HCFs (in red): (a) level walking and (b) stair climbing in anterior-posterior direction and (c) level walking and (d) stair climbing in lateral-medial direction

Fig 4. Comparison between the predicted muscle forces and EMG profiles for (a) level walking. (b) climbing stairs. The red and black line represent the EMG profile and forces in each muscle bundle respectively.

Fig 5. The predicted HJC translation (solid line) with SD for (a) level walking and (b) climbing stairs for three subjects.

Fig 6. The comparsion between average values of predicted hip joint center translation (black dash line) and experimental results (color solid line) from dual fluoroscope imaging system under same acetabluar coordinate system.

Fig 7. Bland-Altmen's plots between FDK approach and experimental measurements. (a) The difference-average analysis of level walking. (b) The difference-average analysis of climbing stairs. (c) The ratio-average analysis of level walking. (d) The ratio-average analysis of climbing stairs.

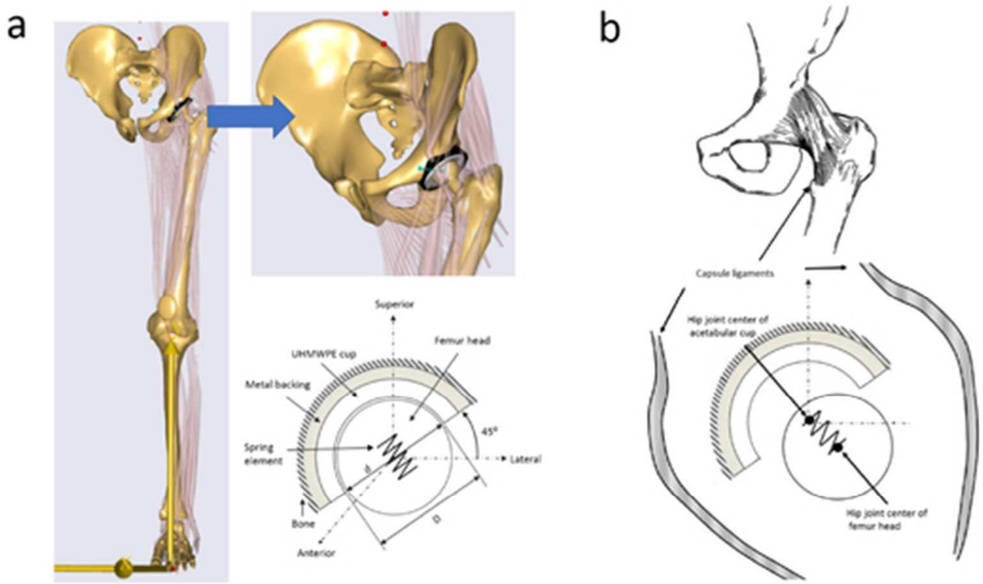

Fig 1. The schematic of MSK model by the FDK approach. (a) The FDK approach provided three additional translation DOFs in hip joint (anterior-posterior, superior-inferior and medial-lateral direction). (b) A linear spring element was used to simulate the passive function of capsule ligaments.).
44x26mm (300 x 300 DPI)

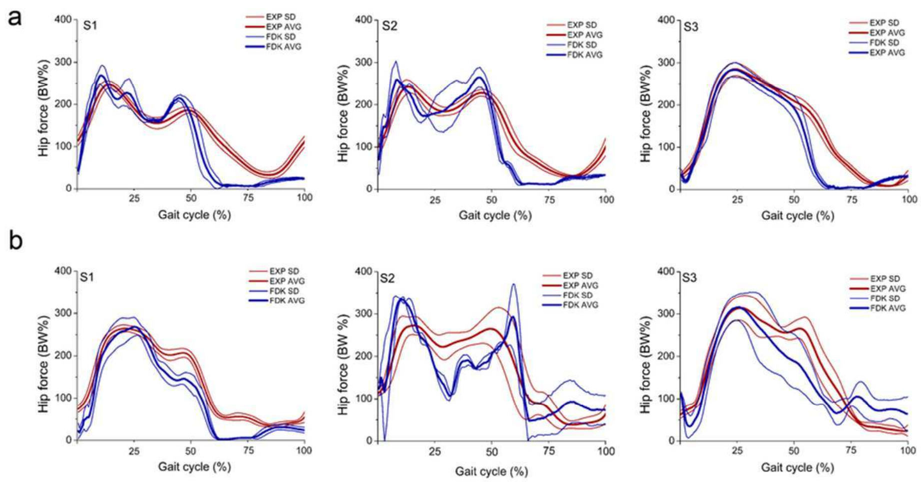

Fig 2. Comparison between the HCFs of FDK approach (in blue) and experimental HCFs (in red) for (a) level walking and (b) stair climbing.
84x45mm (300 x 300 DPI)

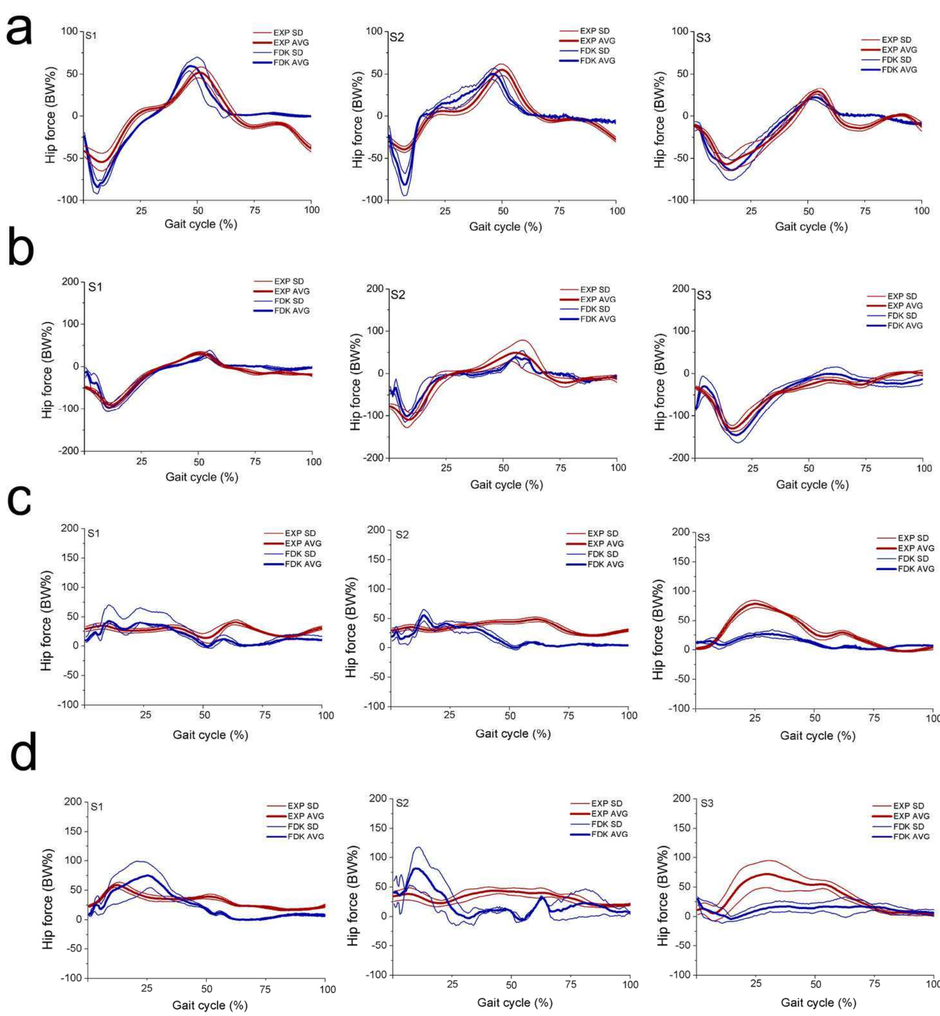

Fig 3. Comparison between the HCFs of FDK approach (in blue) and experimental HCFs (in red): (a) level walking and (b) stair climbing in anterior-posterior direction and (c) level walking and (d) stair climbing in lateral-medial direction

84x90mm (600 x 600 DPI)

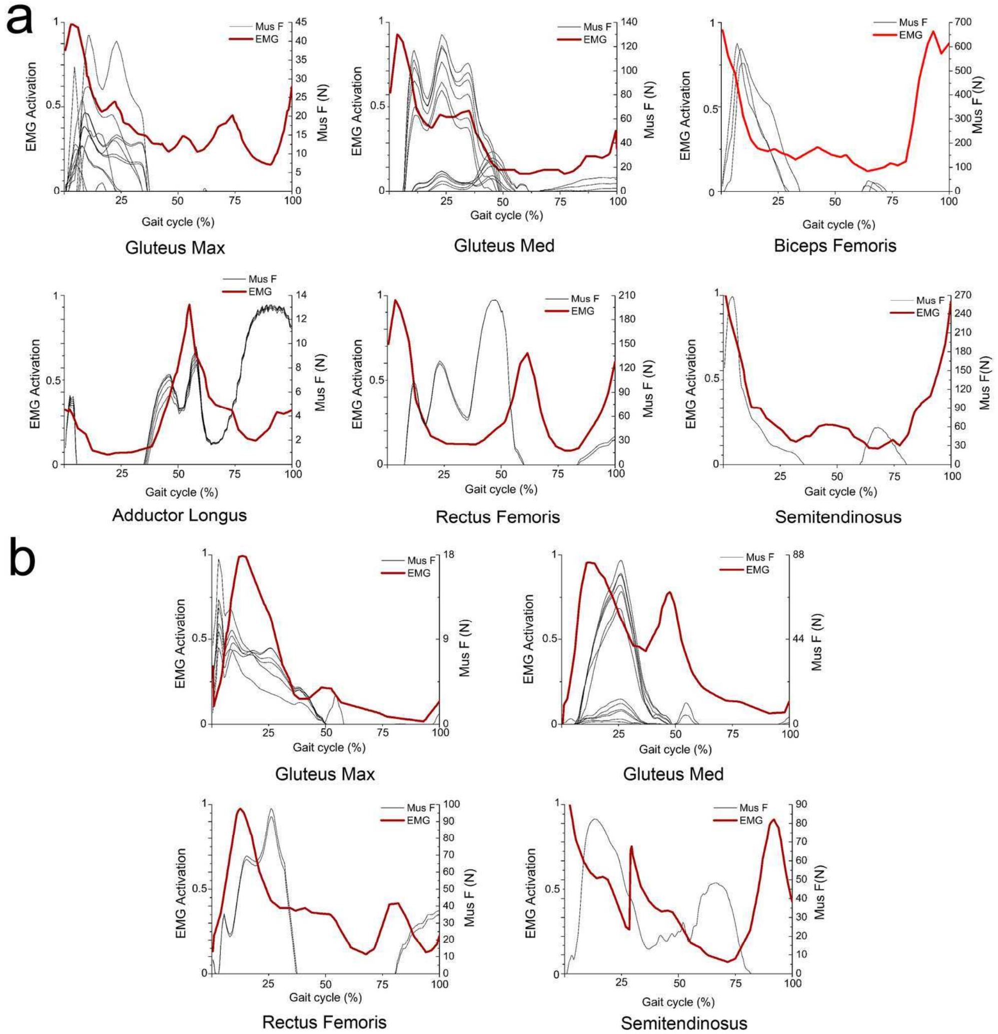

Fig 4. Comparison between the predicted muscle forces and EMG profiles for (a) level walking. (b) climbing stairs. The red and black line represent the EMG profile and forces in each muscle bundle respectively.

84x90mm (600 x 600 DPI)

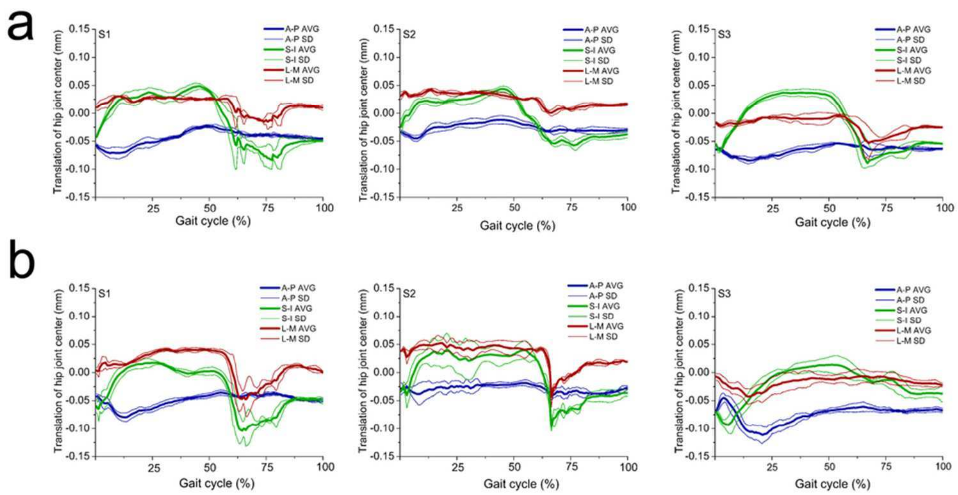

Fig 5. The predicted HJC translation (solid line) with SD for (a) level walking and (b) climbing stairs for three subjects.
42x22mm (600 x 600 DPI)

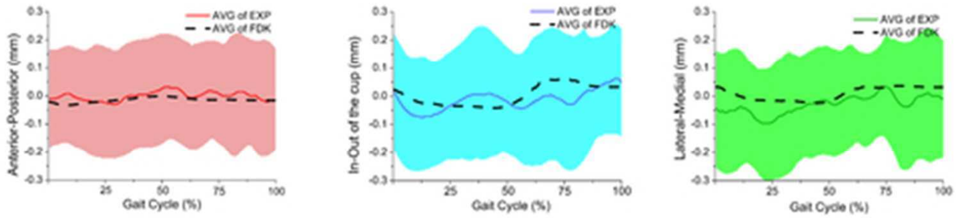

Fig 6. The comparsion between average values of predicted hip joint center translation (black dash line) and experimental results (color solid line) from dual fluoroscope imaging system under same acetabluar coordinate system.
21x5mm (600 x 600 DPI)

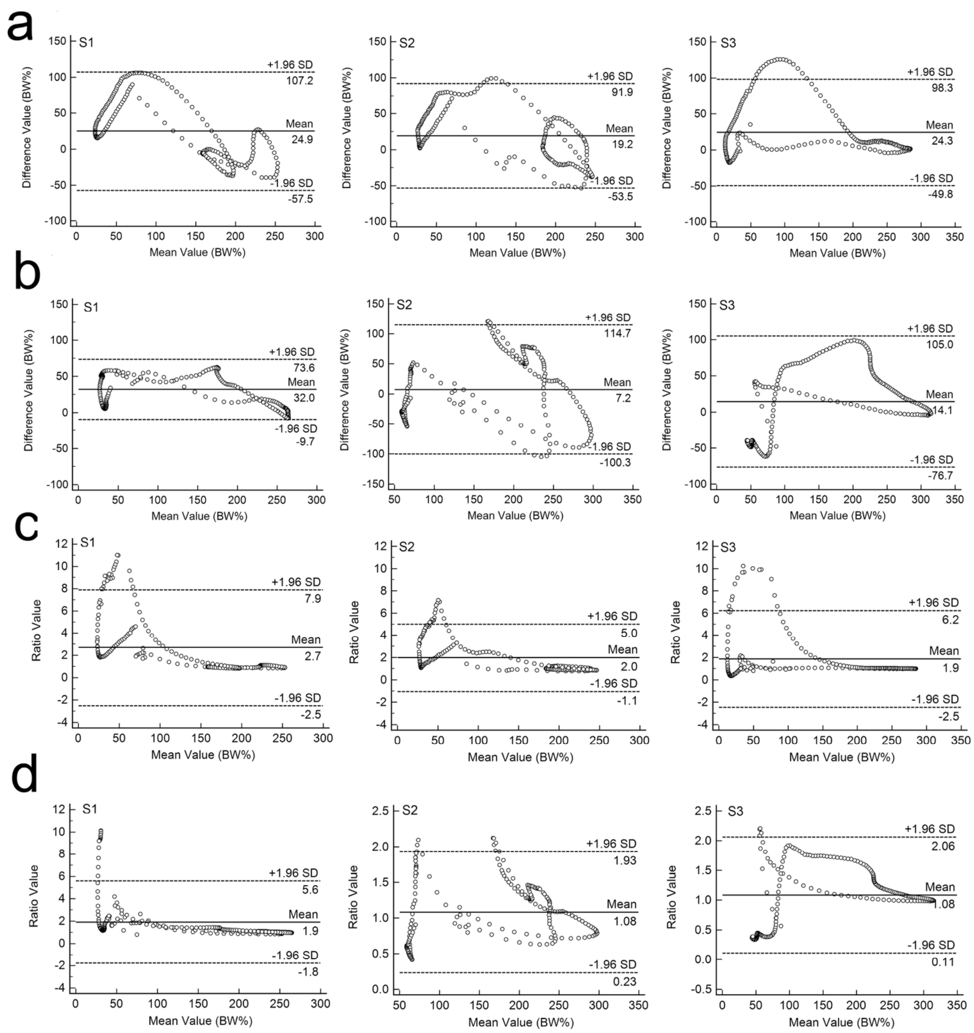

Fig 7. Bland-Altmen's plots between FDK approach and experimental measurements. (a) The difference-average analysis of level walking. (b) The difference-average analysis of climbing stairs. (c) The ratio-average analysis of level walking. (d) The ratio-average analysis of climbing stairs.
84x90mm (600 x 600 DPI)

Table 1. Characteristic of patients and the experimental trials available in the Hip 98 database.

Subject	Hip 98 name	Sex	Age	Body weight(N)	Height(m)	Level walking	Stairs climbing
S1	HSR	M	55	860	1.74	8 trials	6trials
S2	KWR	M	61	702	1.65	8 trials	6trials
S3	IBL	F	76	800	1.70	5 trials	6trials

Table 2. Sensitivity of hip contact forces to changes in muscle recruitment criterion and material parameter *PressureModule* during normal gait cycle (Sample: HSR). '*' means the nominal value for investing the effect of model parameters on hip contact forces by relative deviation of peak value (RDPV) and mean trial deviation. More details on parameter description of the model can be found in AnyBody manual

Model parameters	Parameter description	Total walking		Total climbing	
		RDPV (%)	**Mean trial deviation (BW %)**	**RDPV (%)**	**Mean trial deviation (BW %)**
Muscle recruitment criterion: Quadratic polynomial *	distribute the load between several muscles in various polynomial forms with power 2				
Cubic polynomial	distribute the load more evenly between muscles in various polynomial forms with power 3	5.79	11.35	5.23	10.75
Min/Max	distributes the collaborative muscle forces in such a way that the maximum relative muscle force is as small as possible	12.47	17.58	10.53	15.98
PressureModule: Max $4.42 \times 10^{11} N/m^3$	The value corresponding to the UHMWPE cup thickness of 5.72 mm	0.78	2.56	0.92	3.42
Min $2.56 \times 10^{11} N/m^3$	The value corresponding to the UHMWPE cup thickness of 14.11 mm	0.52	1.33	0.60	1.82
$2.88 \times 10^{11} N/m^3$ *	The value corresponding to average thickness of 7.60 mm				

Table 3. Relative deviation of peak value, mean of trial deviation and RMSE value between average trials of predicted HCF (FDK approach) and experimental value.

Activity	Subject	Relative deviation of peak value (% of EXP value)	Mean trial deviation (BW %)	RMSE (BW %)
Level walking	S1	8.65	-24.91	48.72
	S2	9.10	-19.17	41.67
	S3	-0.46	-24.21	44.84
Climbing stairs	S1	1.46	-31.98	38.36
	S2	22.57	-7.19	55.17
	S3	0.58	-14.13	48.36

Note:The negative value indicated that the predicted value was underestimated than the experimental value

Table 4.Mean of trial deviation and RMSE value of predicted HCFs in anterior-posterior (A-P) and lateral-medial (L-M) directions.

Activity	Subject	Mean trial deviation of FDK approach (BW %)		RMSE (BW %)	
		A-P	L-M	A-P	L-M
Level walking	S1	1.27	-8.93	15.63	15.86
	S2	0.32	-17.75	14.19	24.72
	S3	0.72	-18.72	8.07	27.73
Climbing stairs	S1	11.34	-6.51	26.50	28.56
	S2	1.04	-11.10	15.48	26.39
	S3	-2.00	-22.83	15.65	32.92

Note:The negative value indicated that the predicted value was underestimated than the experimental value

Appendix

Table A. Sensitivity analysis of the influence of modelling parameters on HCFs, in terms of relative deviation of peak value (RDPV) and mean trial deviation. Different values of each parameters were adopted during a cycle with respect to nominal conditions (Muscle recruitment: Quadratic polynomial, PressureModule: $2.88x10^{11}N/m^3$, Spring stiffness: $5×10^4$ N/m, Type of actuator: Piecewise Linear).

Model parameters	One walking cycle		One climbing stairs cycle	
	RDPV (%)	Mean trial deviation (BW %)	RDPV (%)	Mean trial deviation (BW %)
Spring stiffness				
$5x10^2$N/m	0.06	-0.04	0.06	-0.07
$5x10^3$N/m	0.07	-0.04	0.06	-0.07
Type of actuator	**RDPV (%)**	**Mean trial deviation (BW %)**	**RDPV (%)**	**Mean trial deviation (BW %)**
Bezier	1.66	-1.34	-5.59	1.03

Table B. Sensitivity analysis of the influence of modelling parameters on HJC translation, in terms of relative deviation of peak value (RDPV) and mean trial deviation. Different values of each parameters were adopted during a cycle with respect to nominal conditions (Muscle recruitment: Quadratic polynomial, PressureModule: $2.88x10^{11}N/m^3$, Spring stiffness: $5×10^4$ N/m, Type of actuator: Piecewise Linear).

Model parameters	**A-P**			**S-I**			**L-M**		
Muscle recruitment	**RDPV (%)**	**Mean trial deviation (mm)**		**RDPV (%)**	**Mean trial deviation (mm)**		**RDPV (%)**	**Mean trial deviation (mm)**	
Level walking		**stance**	**swing**		**stance**	**swing**		**stance**	**swing**
Cubic polynomial	1.65	0.0005	-0.0010	-7.32	0.0019	-0.0107	-9.96	0.0028	-0.0115
Min/Max	1.32	0.0018	-0.0016	-13.49	0.0069	-0.0185	-16.54	0.0073	-0.0205
Climbing stairs									
Cubic polynomial	1.34	-0.0005	-0.0008	-8.38	0.0016	-0.0152	-15.64	0.0028	-0.0153
Min/Max	4.56	-0.0007	-0.0013	-9.86	0.0051	-0.0196	-20.24	0.0088	-0.0224
PressureModule	**RDPV (%)**	**Mean trial deviation (mm)**		**RDPV (%)**	**Mean trial deviation (mm)**		**RDPV (%)**	**Mean trial deviation (mm)**	
Level walking									
$2.88x10^{11}N/m^3$	-6.53	0.0002	0.0007	8.32	-0.0092	0.0110	11.53	-0.0036	0.0095
$4.42x10^{11}N/m^3$	-9.95	0.0002	0.0014	15.13	-0.0167	0.0185	14.55	-0.0072	0.0126
Climbing stairs									
$2.88x10^{11}N/m^3$	-2.30	0.0016	0.0004	7.16	-0.0090	0.0109	11.63	-0.0043	0.0123
$4.42x10^{11}N/m^3$	-3.29	0.0031	0.0007	10.55	-0.0152	0.0157	13.80	-0.0077	-0.0172
Spring stiffness	**RDPV (%)**	**Mean trial deviation (mm)**		**RDPV (%)**	**Mean trial deviation (mm)**		**RDPV (%)**	**Mean trial deviation (mm)**	
Level walking									
$5x10^2N/m$	0.10	N/A	0.0001	2.26	N/A	0.0011	7.01	N/A	0.0013
$5x10^3N/m$	0.11	N/A	0.0001	2.67	N/A	0.0015	7.22	N/A	0.0013
Climbing stairs									
$5x10^2N/m$	0.01	N/A	0.0002	3.37	N/A	0.0069	7.91	N/A	0.0061
$5x10^3N/m$	0.01	N/A	0.0002	3.54	N/A	0.0072	8.35	N/A	0.0064
Type of actuator	**RDPV (%)**	**Mean trial deviation (mm)**		**RDPV (%)**	**Mean trial deviation (mm)**		**RDPV (%)**	**Mean trial deviation (mm)**	
Level walking									
Bezier	-1.39	0.0002		-6.33	0.0036		-14.25	0.0031	
Climbing stairs									
Bezier	1.91	N/A		-9.03	0.0025		-16.29	0.0065	

Table C. Sensitivity analysis of the influence of muscle insertion points on HCFs, in terms of relative deviation of peak value (RDPV) and mean trial deviation.

Muscle	Deviation of insertion point	RDPV (%)	Mean trial deviation (BW %)
Gluteus Med	5mm	-0.01 – 0.01	-0.01 – 0.01
	10mm	**-0.17 – 6.39**	**-5.45 – 2.94**
Adductor Lonugs	5mm	-0.01 – 0.01	-0.01 – 0.01
	10mm	**-3.43 – 0.10**	**-0.48 – 0.08**
Biceps Femoris	5mm	-0.01 – 0.01	-0.01 – 0.01
	10mm	**-0.03 – 0.20**	**-0.21 – 0.26**
Semitendinosus	5mm	-0.01 – 0.01	-0.01 – 0.01
	10mm	-0.01 – 0.01	-0.01 – 0.01

Table D. Sensitivity analysis of the influence of muscle insertion points on HJC translation, in terms of relative deviation of peak value (RDPV) and mean trial deviation.

Muscle	Deviation of insert point	A-P		S-I		L-M	
		RDPV (%)	Mean Trial Deviation (mm)	RDPV (%)	Mean Trial Deviation (mm)	RDPV (%)	Mean Trial Deviation (mm)
Gluteus Med	5mm	-0.01– 0.01	-0.001 – 0.001	-0.01 – 0.01	-0.001 – 0.001	-0.01 – 0.01	-0.001 – 0.001
	10mm	**-1.29 – 1.88**	-0.001 – 0.001	**-0.70 – 0.38**	-0.001 – 0.001	**-9.16 – -1.01**	-0.001 – 0.001
Adductor Longus	5mm	-0.01 – 0.01	-0.001 – 0.001	-0.01 – 0.01	-0.001 – 0.001	-0.01 – 0.01	-0.001 – 0.001
	10mm	-0.01 – 0.01	-0.001 – 0.001	**-0.13 – 0.16**	--0.001 – 0.001	**-2.23 – 2.12**	-0.001 – 0.001
Biceps Femoris	5mm	-0.01 – 0.01	-0.001 – 0.001	-0.01 – 0.01	-0.001 – 0.001	-0.01 – 0.01	-0.001 – 0.001
	10mm	**-0.55 – 0.25**	-0.001 – 0.001	**-0.55 – 0.23**	-0.001 – 0.001	**-0.55 – 0.29**	-0.001 – 0.001
Semitendinosus	5mm	-0.01 – 0.01	-0.001 – 0.001	-0.01 – 0.01	-0.001 – 0.001	-0.01 – 0.01	-0.001 – 0.001
	10mm	-0.01 – 0.01	-0.001 – 0.001	-0.01 – 0.01	-0.001 – 0.001	-0.01 – 0.01	-0.001 – 0.001